

OVERVIEW OF RI-MODE RESULTS ON TEXTOR-94

R. R. WEYNANTS¹, A.M. MESSIAEN¹, J. ONGENA^{1*}, B. UNTERBERG², G. BONHEURE¹, P. DUMORTIER¹, R. JASPERS³, R. KOCH¹, H.R. KOSLOWSKI², A. KRÄMER-FLECKEN², G. MANK², J. RAPP², M.Z. TOKAR², G. VAN WASSENHOVE¹, W. BIEL², M. BRIX², F. DURODIE¹, G. ESSER², K.H. FINKEN², G. FUCHS², B. GIESEN², J. HOBIRK², P. HÜTTEMANN², M. LEHNEN, A. LYSSOIVAN¹, Ph. MERTENS², A. POSPIESZCZYK², U. SAMM², M. SAUER², B. SCHWEER², R. UHLEMANN², P.E. VANDENPLAS¹, G. VAN OOST¹, M. VERVIER¹, V. PHILIPPS², G. WAIDMANN², G.H. WOLF²

Trilateral Euregio Cluster :

(1) Laboratoire de Physique des Plasmas - Laboratorium voor Plasmafysica, Association "EURATOM-Belgian State" Ecole Royale Militaire- B-1000 Brussels - Koninklijke Militaire School

(2) Institut für Plasmaphysik, Forschungszentrum Jülich GmbH, EURATOM Association , D-52425 Jülich, FRG

(3) FOM Instituut voor Plasmafysica Rijnhuizen Associatie "FOM-EURATOM", Nieuwegein, The Netherlands

Abstract

The radiative improved mode is a tokamak regime offering many attractive reactor features. In this paper the RI-mode of TEXTOR-94 is shown to follow the same scaling as the Linear Ohmic Confinement regime, thus identifying it as one of the most fundamental tokamak operational regimes. The current understanding derived from experiments and modeling of the conditions necessary for sustaining the mode is reviewed as are the mechanisms leading to L- to RI- mode transition. The compatibility of high impurity seeding with the low central power density of a burning reactor is discussed as well as RI-mode properties at and beyond the Greenwald density.

1. INTRODUCTION

In a given device, the dominant scaling parameter for the energy confinement τ in ohmically heated tokamak discharges is the density, as reflected in the Neo-Alcator or Linear Ohmic Confinement (LOC) scaling law

$$\tau_{N.A.} \propto \bar{n} R^2 a q \propto \bar{n} R B a^3 I_p^{-1} \quad (1)$$

where \bar{n} is the central line-averaged density, R and a the major and minor radius respectively and q the safety factor at the plasma boundary, B the toroidal field and I_p the plasma current. In contrast, in auxiliary heated discharges, the density is normally of minor importance and essentially replaced by the plasma current as the main scaling parameter, whereas in addition degradation with increasing power occurs. Examples of these are the ITER L-mode scaling law L-89P, which, for deuterium plasmas and applied to TEXTOR-94 geometry, reads (units : \bar{n} (10^{20} m⁻³), $B(T)$, I_p (MA), P (MW)):

$$\tau_{L89-P} = 0.105 \bar{n}^{-0.10} B^{0.2} I_p^{0.85} P^{-0.50} \text{ (s)}, \quad (2)$$

and the ITER ELM-free H-mode scaling H-93P, which predicts:

* Researcher at FWO Vlaanderen

$$\tau_{H93-P} = 0.22 \bar{n}^{0.17} B^{0.35} I_p^{1.06} P^{-0.67} \quad (s). \quad (3)$$

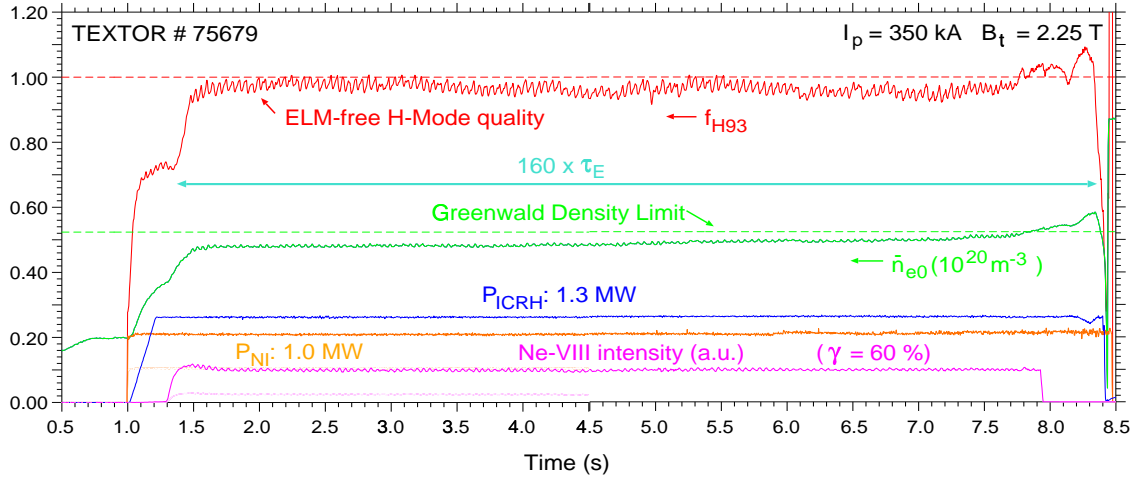


Fig. 1 Temporal evolution of H-mode enhancement factor f_{H93} , line density \bar{n}_e , heating power (ICRH and NBI) and intensity of Ne-VIII line in long pulse RI-M discharge.

The Radiative Improved Mode (abbreviated RI-M) [1-4] is an auxiliary heated regime in which the confinement is improved with respect to the L-mode scaling and which, because it is characterised by the reappearance of the density as the main scaling parameter, permits to obtain confinement as high as H-mode. The qualifier “radiative” refers to the fact that the mode was discovered while establishing the feasibility of the ‘cold plasma mantle’ concept as a means to solve the reactor exhaust problem [5,6]. This RI-M regime allows to produce in TEXTOR-94 simultaneously many highly desirable reactor features: (i) confinement of the quality of ELM-free or ELMy H-mode ($= 0.85$ ELM-free) at densities around the Greenwald density limit, (ii) edge radiation fractions up to 95% of the total input power, (iii) high beta (normalised beta $\beta_n=2$ or poloidal beta $\beta_p=1.5$), i.e. up to the previously observed beta limits of TEXTOR-94, (iv) negligible effect of the seeded impurity on the neutron yield, (v) high values for the figure of merit for ignition margin f_{L89}/q up to 0.80 at high densities. Here, f_{L89} is the enhancement factor of the observed confinement with respect to the scaling expression (2) whereas later on also f_{H93} will be used to denote the enhancement with respect to expression (3). These excellent properties can be stationarily maintained for times as long as the available flux swing. Figure 1 shows such an example sustained for 7s which amounts to 160τ , i.e. the ratio of burn time to confinement time for ITER and longer than the current diffusion time for the discharge concerned.

The present paper presents an overview of the recent developments in the experimental RI-mode program of TEXTOR-94 and of the advances that have been made in the understanding of the nature and the operational requirements of the RI-M.

2. THE CONFINEMENT OF THE RI-MODE

The crosses in Fig. 2 show, plotted versus the normalised density \bar{n}/\bar{n}_{Gr} (or Greenwald number N_{Gr}) where \bar{n}_{Gr} is the Greenwald density ($= I_p/\pi a^2$), the quantity $\tau P^{0.67}/I_p$ for the auxiliary heated discharges (combinations of NBI-co, NBI-cou and ICRH) in the TEXTOR-94 database ($250 < I_p$ (kA) < 500 , $1.7 < B(T) < 2.6$, $a = 0.46$ m, deuterium, boronised walls), in which neon was used as a seeding element to set the radiating mantle. Also shown on this diagram by the circles are the ohmic discharges from which these discharges started. Note however that the neon was only introduced in the auxiliary heated phase of the discharges. For each of the auxiliary heated discharges we have moreover calculated $\tau_{L89} P^{0.67}/I_p$, i.e. using for τ the value given by Eq. (2), and find all these predictions to fall in a domain delineated by the contour marked L-mode. Two straight solid lines are also added to the figure, representing respectively

$$\tau = 0.18 \bar{n} P^{-0.67} \quad (s), \quad \text{and} \quad (4)$$

$$\tau = 0.15 I_p P^{-0.67} \quad (s). \quad (5)$$

The first of these lines passes at the same time through the LOC points and through the highest auxiliary heated discharges (which we qualify as RI-M discharges). The lowest auxiliary heated

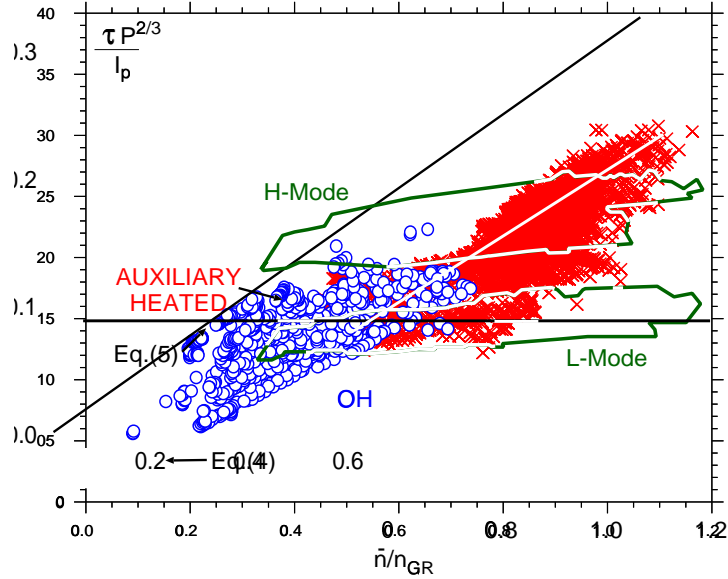


Fig. 2. The TEXTOR-94 database of auxiliary (crosses) and ohmically (circles) heated plasmas plotted in a $(\tau P^{0.67} / I_p, \bar{n}/n_{GR})$ diagramme. The lower contour delineates the domain of the L-mode prediction and the upper one that of the H-mode prediction for the auxiliary heated discharges. Also shown are the lines corresponding to Eqs. (4) and (5).

discharges and the saturated ohmic confinement (SOC) ones are seen to overlap mutually as well as with the domain predicted by the L-mode scaling law, and are (neglecting a weak \bar{n} and B dependence) well approximated by the second line. A last addition to Fig. 2 is the contour marked H-mode which contains the points representing $\tau_{H93} P^{0.67}/I_p$ of the auxiliary heated discharges, confirming that the RI-M surpasses the ELM-free H-mode at a density somewhat below $N_{Gr} = 1$.

It is worthwhile adding that with a freshly siliconised wall the center of gravity of the auxiliary heating shot database decisively shifts away from the L-mode and aligns almost exclusively with the RI-M one. Note finally that Eqs.(4) and (5) pertain only to D injection in D plasmas and that for H into D lower confinement is found [7].

From the data shown in Fig. 2, it would appear that the RI-M and the LOC discharges do not only have a common density dependence [8] but indeed follow the same scaling. For the LOC data this confirms the weaker current dependence (note also that $P \propto I_p$) found earlier on TEXTOR [9] and that the B-dependence on modern day machines [10] appears to be weaker than expressed by Eq. (1). For the RI-M data, Eq. (4) essentially reproduces the earlier RI-M scaling [3, 8] except that specific B-dependence studies have shown the latter also here to be unimportant. The similarity of the scaling in SOC and L-mode was noted before [11]; in TEXTOR-94 they are apparently identical.

These observations lead to the following conclusions: (i) The current dependence in Eq. (1) is also effectively a power one such that ohmic LOC plasmas ‘degrade’ with power. The RI-M is characterised by the same scaling and does not present an extra degradation with respect to the LOC. The fact that Eqs. (4) and (5) have the same power dependence suggests that in all regimes τ decreases when the temperature T increases and that this dependence is of the form T^{-2} . For the LOC - RI-M branch, Eq. (4) suggests that the effective thermal conductivity, which we will call χ_{RIM} , scales as $T^2 n^{-1}$.

(ii) If the identity in scaling implies the same physics, the RI-M database is also the LOC database and actually also the Improved Ohmic Confinement (IOC) database, meaning that obtaining the RI-M out of L-mode might need the same control actions as getting IOC out of SOC. The RI-M is then also not a peculiarity but is one of the most fundamental tokamak modes (LOC - IOC - RI-M), not unexpected [12] but requiring considerable operational skill to achieve with auxiliary heating.

Indeed, to reach by means of RI-M an f_{H93} of at least 0.85 a certain number of control

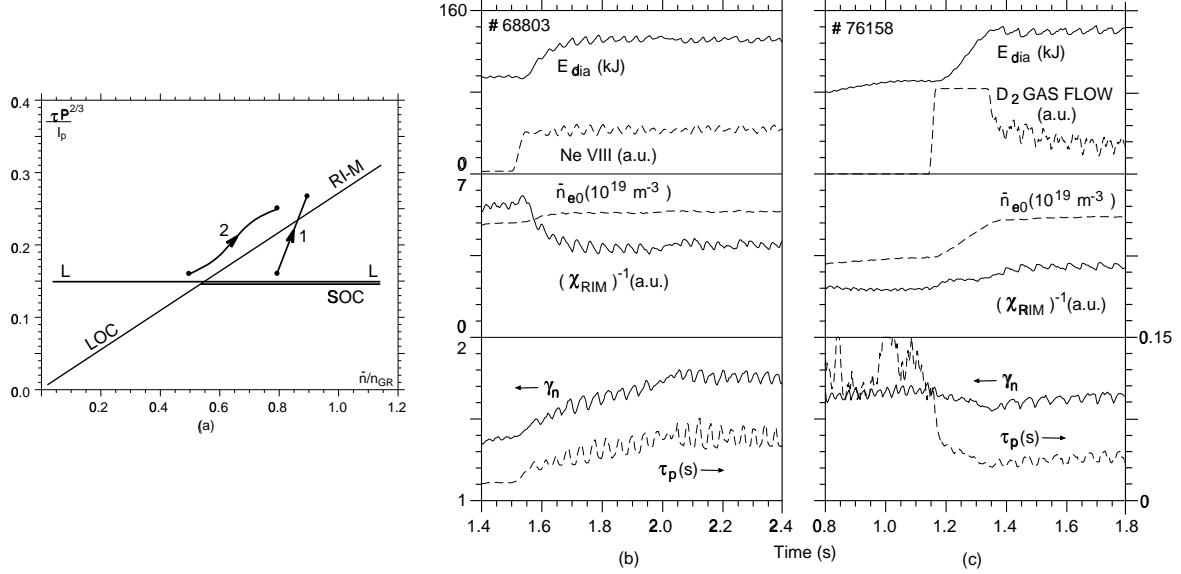


Fig. 3 (a) Schematic version of Fig. 2 with trajectories of discharges of (b) $\equiv 1$ and (c) $\equiv 2$.

(b) Temporal evolution of the energy E_{dia} , neon monitor or gas programming, line density \bar{n}_e , $1/\chi_{RIM}$, the particle confinement time τ_p and the density profile peaking γ_n for discharge 68803 ($I_p = 0.41$ MA, $P = 2.45$ MW, $B = 2.23$ T).

(c) *idem* for discharge 76158 ($I_p = 0.41$ MA, $P = 2.68$ MW, $B = 2.23$ T).

conditions have to be fulfilled: (i) $\gamma = P_{rad}/P > 0.45-0.5$ through the seeding (Ne, Ar) or sputtering (Si) of medium Z impurities; (ii) a density exceeding about 75% of the Greenwald density; (iii) a minimal deuterium co-injection of 20 to 25% of P_{tot} in a deuterium plasma; (iv) an optimum horizontal position depending on the current, toroidal magnetic field, heating scenario and wall condition; (v) low gas puff rate. Please note that in ASDEX [13] neon seeding and low gas feed rates were agents for allowing access from the SOC to the IOC, while SOC only occurs above the Shimomura density [11] which equals $0.5 \bar{n}_{Gr}$. It is also important to note here that in ISX-B it was possible to generate a density dependent scaling in auxiliary heated plasmas by either increased radiation or plasma position displacements [14].

3. UNDERSTANDING THE RI-MODE

The TEXTOR confinement situation can schematically be summarised in Fig. 3a. To aid our understanding of the RI-M we describe the temporal evolution of two model discharges, giving rise to the trajectories 1 and 2. Trajectory 1 is that of a discharge (see Fig. 3b) evolving from L to RI-M as a result of neon injection at high density. The other trajectory traces a discharge with siliconised walls which stays all the time in the RI-M while gas puffing raises the density.

The most salient feature of discharge 1 is the peaking of the density profile (characterised by the ratio γ_n of the central density to the volume averaged density $n(0)/\langle n \rangle$) occurring as the result of the neon injection while f_{H93} rises from 0.72 to 1.03. In discharge 2 (Fig. 3c) f_{H93} rises from 0.65 to 0.95 but γ_n remains practically constant. Note that in discharge 2 the confinement increase tracks the increase in n / T^2 , i.e. in χ_{RIM}^{-1} . As this is not at all the case for discharge 1, one has to conclude that the physical mechanisms leading to confinement improvement are quite different. Also the particle confinement time τ_p evolves quite differently. The high energy phases are both RI-Mode, however, and their values of χ_{RIM} , τ_p and γ_n are quite similar. Note in passing, that, although there is a strong dependence of τ_p on density in the RI-M [15], the particle confinement at the same density is higher in RI-M than in L-mode.

The picture that emerges globally from this type of comparisons is that the RI-M is a regime with peaked profiles and high particle confinement in which the transport is governed by a turbulent mode with an effective $\chi \propto T^2/n$, a prototypical example of which might be the Dissipative

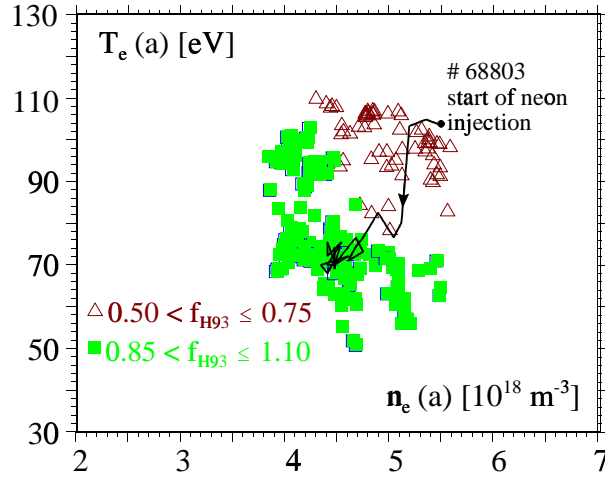


FIG. 4 Edge operational diagram of the RI-mode, different symbols indicating energy enhancement with respect to ELM-free H-mode ($0.80 < N_{Gr} < 1.1$, $2.0 < P < 3.0$ MW). Also shown is the trajectory followed by the discharge of Fig. 3b.

Trapped Electron Mode. Note carefully that a RI-M does not necessarily have to grow out of an L-mode, as demonstrated by trajectory 2. However, when it does so, as is the case in discharge 1, a different turbulent mode must be first quenched before the RI-M can be obtained.

Note furthermore that the true character of the L-mode can only show up where a clear distinction with the RI-M is possible, typically above $N_{Gr} = 0.75$. There, L-mode plasmas from the data base ($f_{H93} < 0.75$) are broad with γ_n of order 1.4-1.6 whereas a RI-M with an f_{H93} of at least 0.9 requires a γ_n of 1.6 or higher (see also Fig. 3). Observations are that both the presence of the NBI-Co beam [16] and the plasma displacements are needed to assure this peaking to be possible.

4. MODELING THE L-MODE TO RI-MODE TRANSITION

Understanding this growth of RI-M out of L-mode requires then to (i) ascertain the mechanism of profile peaking, and (2) identify the mode dominating L-mode confinement. Significant progress has been made on both these scores.

Modeling the density profiles with the RITM code has shown [17] that an essential ingredient for peaking the density profile is the action of the radiative mantle on the anomalous inward pinch v_{in} , which is taken of the form $v_{in} = 1/2 T_e dT_e/dr D$, where D is the perpendicular particle diffusivity. This form can be justified by arguments of profile consistency [18], but more generally as a fundamental off-diagonal contribution of the transport matrix for fluctuation driven particle transport [19]. It was also found to be essential in explaining the SOC-IOC transitions in ASDEX [20]. Impurity seeding lowers the temperature at the edge and steepens the temperature gradient deeper inside the plasma. As at the same time the edge density is found to be lowered or clamped, the neutral ionisation length and the fuelling efficiency increase and the edge diffusivity decreases, effects which all further favor the profile peaking (leading as well to an enhanced τ_p). Typically, the ratio v_{in}/D increases globally by a factor of two. Note that the thus sketched interplay results in the edge plasma properties becoming a sensitive monitor for distinguishing L and RI-M [21]. In Fig. 4 it is seen that discharges in the density range $0.8 < \bar{n}/\bar{n}_{Gr} < 1.1$ have edge densities and edge temperatures at the LCFS which clearly separate according to their L- ($0.5 < f_{H93} < 0.7$) or RI-M-character ($0.85 < f_{H93} < 1.10$). Also shown in this diagram is the trajectory followed by our model discharge (Fig.3b).

The strong increase of τ_p substantially reduces the convective energy losses and is found in simulations by means of RITM and TRANSP to be responsible for up to a quarter of the energy confinement improvement. The major part is however due to a reduction in thermal conductivity. Figure 5 shows the changes in the effective conductivity χ_{eff} (electrons and ions combined) given by TRANSP for the two model discharges of Fig. 3. In both cases χ_{eff} changes over the whole profile. Indications are that the ion channel gets a larger share of the energy increase in Fig. 3b than in Fig.3c. Modeling by means of a nonlinear gyrokinetic particle-in-cell simulation [22] show that in the first discharge the ion thermal flux should drop by a factor 6 on account of a

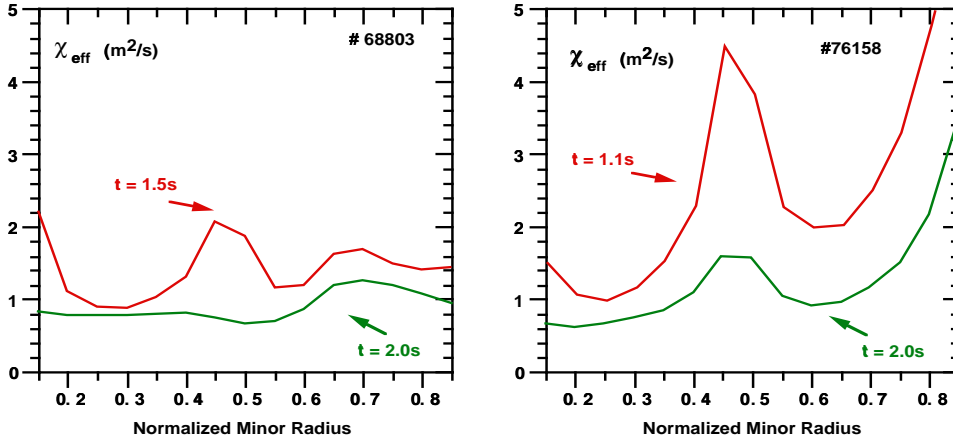


Fig. 5 The effective heat conductivities of (a) discharge 68803 (see Fig. 3b) and (b) discharge 76158 (see Fig. 3c).

reduction of Ion Temperature Gradient (ITG)-Driven turbulence during the evolving density and temperature profiles. These simulations indicate that about 20% of the improvement is a result of the increase of the neon concentration, the rest is to be accounted by the profile changes. ITG-mode suppression is therefore a candidate for the confinement improvement from L to RI-M. It can not be ruled out that the presence of a minimal amount of the NBI-Co injection serves, through sheared toroidal velocity, the additional purpose of enhancing the EXB shear [23], capable of further quenching ITG-modes. The RI-M state can however be achieved without significant EXB shear as it can be sustained with balanced injection [24] and as appears to be suggested by the identity in the scaling of LOC and RI-M plasmas. Note furthermore that ITG was assumed to be suppressed in IOC without rotation [13].

5. IMPORTANT ISSUES FOR RI-MODE

5.1. Impurities

As indicated, a confinement as good as Elmy H-mode requires, at $\bar{n}/\bar{n}_{Gr} > 0.75$, a radiation fraction $\gamma > 0.45-0.50$, achievable through very moderate seeding. If however optimal RI-M confinement ($f_{H93} > 1$) is to be combined with more substantial heat exhaust (say $\gamma > 0.8$), the question automatically arises whether this can be achieved with central impurity levels and concomitant Bremsstrahlung losses P_{Brem} that would be compatible with the rather low central power density of a burning plasma P_α .

In the discharge of Fig. 3b, γ grows from 0.35 to 0.85. Charge exchange recombination spectroscopy measurements [25] show the central carbon concentration to decrease from 0.014 to 0.010 and the central neon one to rise from 0 to 0.009. The central oxygen concentration, found by assuming that the ratio of the oxygen to carbon densities equals the ratio of the fluxes of these elements measured at the ALT-limiter, drops from 0.007 to 0.005. These concentrations combine to give a central deuterium concentration f_{DT} which changes from 0.86 to 0.81. This almost constant dilution can be understood by a partial replacement of the intrinsic impurities by the seeded one, as witnessed by the observed decreases of the fluxes of these elements at the limiter. It is also consistent with the measured behaviour of the neutron yield in this and other discharges [26]. The central effective charge Z_{eff} increases however, as a result of the replacement of low Z by higher Z elements, from 1.8 to 2.5, values which are confirmed by resistivity measurements.

While such an increase in Z_{eff} raises the central P_{brem} , one should note that the important reactor quantity is $P_{Brem}/P_\alpha \propto Z_{eff}/(f_{DT}^2 T_e^{1.5})$. An increased Z_{eff} and dilution is compensated by the concomitant RI-M confinement improvement which allows to achieve at the same density a strongly increased T_e . It remains important to note however that the low central dilution is the result of the development of a hollow distribution of the impurity concentration over the plasma radius [27]. Simulations by RITM can only reproduce this feature by discarding any anomalous inward impurity pinch (which, as argued before, is essential for the main ions) and retaining only a neo-classical one exhibiting temperature screening in the Pfirsch-Schlüter-regime in the outer

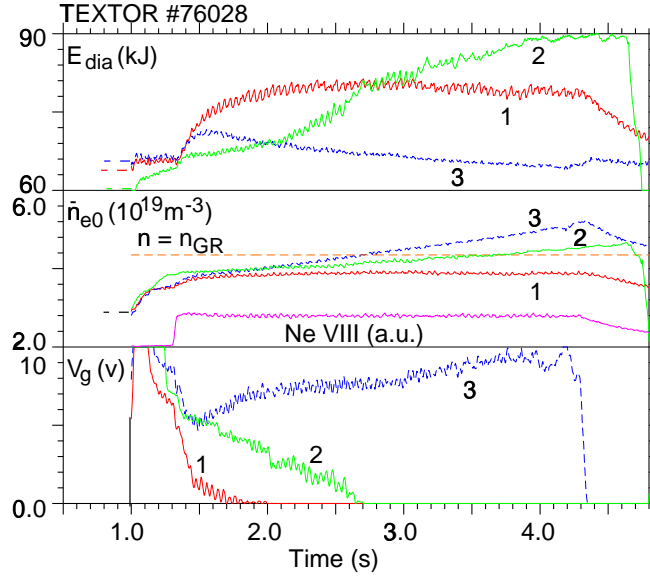


Fig. 6 Temporal evolution of plasma energy E_{dia} and line density \bar{n}_e , for different gas valve programming ($I_p = 0.29$ MA, TEXTOR shots (1) 75994, (2) 76028, (3) 75995).

half of the plasma. The confirmation of this property on other, larger devices constitutes a decisive step for the heat exhaust prospects of a possible RI-M reactor.

5.2. Beta-limit and Greenwald limit

L-mode and RI-M discharges have the same beta-limit. For high and medium currents, the plasma beta is limited at a normalised toroidal $\beta_n = 2$. Attempts to go over this limit result in back-transitions (sudden loss of confinement) triggered by MHD activity, mainly around the $q = 1.5$ surface and which grows up within a few ms before the back-transition. At very low current, the poloidal beta seems to be limiting ($\beta_p = 1.5$ to 1.6).

Studying the density limit in the RI-mode is of paramount importance because of the confinement scaling with density. Experimentally it is found that in RI-M discharges the Greenwald density ($N_{Gr} = 1$) is a rather stringent constraint: N_{Gr} up to 1.05 can be stationary maintained; transiently $N_{Gr} = 1.20$ is possible but a minor or major disruption follows. Note also that these assertions pertain to discharges in which the external gas feed is either strongly reduced or totally absent. With gas puffing, $N_{Gr} = 1$ can be more readily overcome, but at the expense of a strongly degraded confinement. These results are illustrated in Figure 6, where three discharges with $N_{Gr} \approx 1$ are compared. The heating power is 1.75 MW in all cases and the common initial density is $3.0 \cdot 10^{19} \text{ m}^{-3}$ ($N_{Gr} = 0.66$). At $t = 1$ s, the gas valve opens in response the valve voltage V_g , itself feedback controlled to reach a preset total number of particles in the discharge, and the density rises accordingly. At $t = 1.3$ s, neon is injected to set up RI-M conditions. Discharge 1 sets the stationary reference: $N_{Gr} = 0.9$, $f_{H93} = 0.95$, $V_g = 0$ from 1.8 s on. Discharge 2 rises to $N_{Gr} = 1.05$, $f_{H93} = 1.13$ after the closure of the valve. Please note the strongly reduced energy as long as the valve is open and the disruptive end of the discharge. Discharge 3 has the gas valve open all the time, allowing the density to rise to $N_{Gr} = 1.17$ but with f_{H93} dropping to 0.67 and with very flattened density profiles (not shown).

6. CONCLUSIONS

The RI-Mode in TEXTOR-94 has been shown to obey the same confinement scaling as the Linear Ohmic Confinement regime, which allows to identify it as one of the most fundamental tokamak modes, the LOC - IOC - RI-M regime. With the IOC-mode, the RI-M has not only its scaling in common, but also many recipes that are essential for its attainment. A crucial ingredient turns out to be the creation of appropriate wall conditions assuring reduced recycling combined with high fuelling efficiency from the walls, made possible by adequate wall preparation techniques studied over many years on TEXTOR. This turns out to be especially useful for

achieving high density operation without passing at any time through L-mode conditions, such as is the case with fresh siliconisation.

Because of its density dependent scaling, the full confinement quality is attained at high density, close to or above the Greenwald density, where most H-mode plasmas show degraded confinement. To fully realise this potential reactor advantage of the RI-M it becomes of utmost importance to establish the size dependence of the RI-M scaling law and to confirm the favorable radial impurity distribution on larger devices. It is equally important to try to extend the optimal RI-M confinement beyond the hitherto achieved and already high densities.

REFERENCES

1. MESSIAEN, A.M., ONGENA, J., SAMM, U., et al., Nucl. Fusion **34** (1994) 825.
2. MESSIAEN, A.M., ONGENA, J., SAMM, U., et al., Phys. Rev. Lett. **77** (1996) 2487.
3. ONGENA, J., et al., Overview of experiments with radiative cooling at high confinement and high density in limited and diverted discharges, invited paper at 24th Eur. Conf., on Control. Fusion and Plasma Physics, Prague, 1998, to be published in Plasma Phys. Control. Fusion.
4. VANDENPLAS, P.E., MESSIAEN, A.M., ONGENA, J., et al., J. Plasma Phys. **59** (1998) 587.
5. SAMM, U., BERTSCHINGER, G., BOGEN, P., et al., Plasma Phys. Control. Fusion **35** (1993) B 167.
6. WINTER, J., ESSER, H.G., JACKSON, G.L., et al., Phys. Rev. Lett. **71** (1993) 1549.
7. MESSIAEN, A.M., ONGENA, J., UNTERBERG, B., et al., Extended parametric study of the RI-mode on TEXTOR-94, contributed paper at 24th Eur. Conf., on Controlled Fusion and Plasma Physics, Prague, 1998,
8. MESSIAEN, A.M., ONGENA, J., UNTERBERG, B., et al., Comments Plasma Phys. Control. Fusion, **18** (1997) 221.
9. WEYNANTS, R.R., JADOUL, M., MESSIAEN, A.M., et al., in Controlled Fusion and Plasma Physics, (Proc. 14th Eur. Conf. Madrid, 1987), Vol. 11D, Part I, European Physical Society (1987) 197.
10. BARTIROMO, R., in Controlled Fusion and Plasma Physics, (Proc. 18th Eur. Conf. Berlin, 1991), Vol. 15C, Part I, European Physical Society (1991) 73.
11. SHIMOMURA, Y., et al., Empirical scaling of energy confinement time in L-mode plasma and optimised mode and some consideration of reactor core plasma in tokamak, Rep. JAERI-M 85-080, Japanese Atomic Energy Research Institute (1985).
12. KADOMTSEV, B.B., Tokamak Plasma: A Complex Physical System, IOP Publishing, Bristol (1992) p. 141.
13. BESSENROTH-WEBERPALS, M., McCORMICK, K., SÖLDNER, F.X., et al., Nucl. Fusion **31** (1991) 155.
14. WOOTTON, A.J., BUSH, C.E., EDMONDS, P.H., et al., Nucl. Fusion **25** (1985) 479.
15. MESSIAEN, A.M., ONGENA, J., UNTERBERG, B., et al., Phys. Plasmas **4** (1997) 1690.
16. MESSIAEN, A.M., ONGENA, J., UNTERBERG, B., et al., in RF Power in Plasmas (Proc. 12th Topical Conf. Savannah, 1997) AIP Conf. Proc. 403, Ed. P. Ryan & T. Intrator (1997) 41.
17. MESSIAEN, A.M., ONGENA, J., SAMM, U., et al., Nucl. Fusion **36** (1996) 39.
18. TOKAR', M.Z., JASPERS, R. and UNTERBERG, B., Contrib. Plasma Phys. **38** (1998) 67.
19. SHAIN, K.C., Phys. Fluids **31** (1988) 2249.
20. BECKER, G., Nucl. Fusion **30** (1990) 2285.
21. UNTERBERG, B., BRIX, M., JASPERS, R., et al., Plasma wall interaction and plasma edge properties with radiating cooling and improved confinement in TEXTOR-94, 13th Int. Conf. on Plasma Surf. Interact. in Cont. Fus. Devices, San Diego 1998, to be published in J. Nucl. Mater.
22. SYDORA, R., private communication.
23. TOKAR', M. Z., JASPERS, R., and UNTERBERG, B., Nucl. Fusion **38** (1998) 961.
24. JASPERS, R., WIDDERSHOVEN, H.L.M., UNTERBERG, B., et al., The role of velocity shear in the TEXTOR-94 Radiative Improved Mode, 25th Eur. Conf. Prague, 1998, to be published.
25. JASPERS, R., BUSCHE, E., KRAKOR, T., et al., in Controlled Fusion and Plasma Physics, (Proc. 24th Eur. Conf. Berchtesgaden, 1997), Vol. 21A, Part IV, European Physical Society (1997) 1713.
26. VAN WASSENHOVE, G., HELBING, S., BONHEURE, G., et al., *ibidem*, p. 1697.
27. UNTERBERG, B., MESSIAEN, A.M., ONGENA, J., et al., Pl. Phys. Contr. Fus. **39** (1997) 189.